Appl Microbiol Biotechnol (2010) 88:143–153
DOI 10.1007/s00253-010-2734-9

BIOTECHNOLOGICALLY RELEVANT ENZYMES AND PROTEINS

Structural and biochemical characterization of a nitrilase from the thermophilic bacterium, *Geobacillus pallidus* RAPc8

Dael S. Williamson · Kyle C. Dent · Brandon W. Weber · Arvind Varsani · Joni Frederick · Robert N. Thuku · Rory A. Cameron · Johan H. van Heerden · Donald A. Cowan · B. Trevor Sewell

Received: 14 April 2010 / Revised: 9 June 2010 / Accepted: 9 June 2010 / Published online: 4 July 2010

Abstract *Geobacillus pallidus* RAPc8 (NRRL: B-59396) is a moderately thermophilic gram-positive bacterium, originally isolated from Australian lake sediment. The *G. pallidus* RAPc8 gene encoding an inducible nitrilase was located and cloned using degenerate primers coding for well-conserved nitrilase sequences, coupled with inverse PCR. The nitrilase open reading frame was cloned into an expression plasmid and the expressed recombinant enzyme purified and characterized. The protein had a monomer molecular weight of 35,790 Da, and the purified functional enzyme had an apparent molecular weight of ~600 kDa by size exclusion chromatography. Similar to several plant nitrilases and some bacterial nitrilases, the recombinant *G. pallidus* RAPc8 enzyme produced both acid and amide products from nitrile substrates. The ratios of acid to amide produced from the substrates we tested are significantly different to those reported for other enzymes, and this has implications for our understanding of the mechanism of the nitrilases which may assist with rational design of these enzymes. Electron microscopy and image classification showed complexes having crescent-like, "c-shaped", circular and "figure-8" shapes. Protein models suggested that the various complexes were composed of 6, 8, 10 and 20 subunits, respectively.

Keywords Nitrilase · *Geobacillus pallidus* · Tetrahedral intermediate

Electronic supplementary material The online version of this article (doi:10.1007/s00253-010-2734-9) contains supplementary material, which is available to authorized users.

D. S. Williamson · K. C. Dent · B. W. Weber · A. Varsani · R. N. Thuku · B. T. Sewell (✉)
Electron Microscope Unit, University of Cape Town,
Rondebosch, Cape Town 7701, South Africa
e-mail: trevor.sewell@uct.ac.za

K. C. Dent · J. Frederick · R. N. Thuku · J. H. van Heerden
Department of Molecular and Cell Biology,
University of Cape Town,
Rondebosch, Cape Town 7701, South Africa

J. Frederick
Enzyme Technologies, CSIR Biosciences,
Ardeer Road, Modderfontein 1645, South Africa

D. S. Williamson · R. A. Cameron · D. A. Cowan
Institute for Microbial Biotechnology and Metagenomics,
Department of Biotechnology, University of the Western Cape,
Bellville, South Africa

A. Varsani
School of Biological Sciences, University of Canterbury,
Ilam, Christchurch 8140, New Zealand

Introduction

Nitrilases (EC 3.5.5.1) convert nitriles to the corresponding carboxylic acids and ammonia. However, several plant (Piotrowski et al. 2001) and some bacterial nitrilases (O'Reilly and Turner 2003; Brady et al. 2006) have been identified which convert nitriles to both acid and amide products (Fernandes et al. 2006). Nitrilases typically occur as homo-oligomers with a monomer size of around 40 kDa. Activity is usually dependant on subunit assembly, a process affected by temperature, pH, enzyme concentration, and in some instances, the presence of a substrate (O'Reilly and Turner 2003).

Members of the nitrilase superfamily occur in both eukaryotic and prokaryotic species (Pace and Brenner 2001). Nitrilase-related enzymes are characterized by monomers having a conserved $\alpha\beta\beta\alpha$-fold which associate

in a consistent fashion to form dimers. In different members of the superfamily, these dimers associate in different ways to form oligomeric complexes. In the case of nitrilases, these oligomeric complexes are often spirals or helices. A further feature characterizing the nitrilases is the conserved Cys, Glu, Lys catalytic triad which is implicated in covalent catalysis in which the substrate binds to the cysteine (Pace and Brenner 2001; Brenner 2002). It has recently been suggested that this triad includes an additional, structurally conserved Glu residue which is not immediately apparent from sequence conservation, thereby forming a catalytic tetrad (Kimani et al. 2007; Thuku et al. 2009). The nitrilase reaction is thought to be catalysed via covalent thioimidate and thioester intermediates and the release of an amide is not generally observed. However, it has been noted that the difference between ammonia release and amide release from the tetrahedral intermediate formed following the hydrolysis of the thioimidate involves the breakage of either the N–C bond or the S–C bond, and that this may be dependent on rather small differences in the local electronic environment (Jandhyala et al. 2005).

Members of the "true" nitrilase branch of the superfamily exhibit amino acid sequence identity in the region of 30% and display considerable variation in substrate specificity (O'Reilly and Turner 2003). In consequence, members of this branch have been subcategorized according to differences in catalytic properties. Cyanide degrading nitrilases (or cyanide dihydratases) function identically to nitrilase enzymes but efficiently hydrolyze only inorganic cyanide; as opposed to aliphatic and aromatic nitrilases which have a broad organic cyanide substrate range (O'Reilly and Turner 2003). Cyanide hydratases are a subgroup of the nitrilase branch and convert HCN to formamide only demonstrating the principle that these enzymes can function as pure nitrile hydratases (Sosedov et al. 2010).

Nitrilases are potentially useful industrial catalysts, especially in production of low volume, high-cost enantiomeric fine chemicals (Brady et al. 2004, 2006). The enantio- and regio-selective characteristics of these biocatalysts can potentially be exploited to increase their applications in chemical synthesis (Brady et al. 2004).

Previously, a nitrilase from a moderately thermophilic gram-positive bacterium *Bacillus* sp. DAC521 had been purified and shown to have a relative molecular mass of 600 kDa (Almatawah et al. 1999). SDS-PAGE showed the monomer size to be approximately 41 kDa, which suggested that the enzyme formed 15-mer functional complexes. These estimates were, however, potentially obscured by the co-purification of a putative GroEL homologue which interfered with relative mass estimates (Almatawah et al. 1999).

We have identified and sequenced a putative nitrilase-encoding open reading frame (ORF) in a closely related organism, *Geobacillus pallidus* RAPc8 (Pereira et al. 1998). Analysis of the 972 bp sequence confirmed the presence of functional motifs, including a putative Glu, Lys, Cys catalytic triad, that are characteristic of nitrilases. Here, we report the cloning, expression and detailed structural characterisation of the purified recombinant *G. pallidus* RAPc8 nitrilase.

Material and methods

Cloning of the *G. pallidus* RAPc8 nitrilase gene

A pair of degenerate primers was designed against nitrilase consensus regions identified in a multiple alignment of ten bacterial, archaeal and eukaryotic nitrilases. Primer NIT1 (5′-TTY CCN GAR RYN TTY ATM CCN GGN TAY CC-3′) was designed against the conserved region FPEXFIPGYP. Primer NIT3 (5′-GAN CCR TCN CCN TCN CCC CA-3′) was designed against the conserved region WG(D/E)G(D/N)GS. Using *G. pallidus* RAPc8 genomic DNA as a template, these primers were used to polymerase chain reaction (PCR) amplify an internal portion of the nitrilase gene. PCR reaction conditions were: 94°C, 4 min; 25 cycles of 94°C, 30 s; 60°C, 30 s; 72°C, 30 s, and 72°C, 5 min. PCR products were separated by gel electrophoresis and bands in the expected size range (~300 bp) were excised, purified and cloned into pGEM®-T Easy Vector Systems Kit (Promega, USA) to produce plasmid pNIT2.

The pNIT2 insert was excised and labelled using the random prime DIG DNA labelling and detection kit (Roche, Germany). The labelled probe was used in a Southern blot against *G. pallidus* RAPc8 genomic DNA digested with several common restriction enzymes. The Southern blot showed hybridising bands at ~4 kb with both *Eco*RI and *Hind*III digested DNA.

The region containing the putative nitrilase gene was amplified using inverse PCR with two primers, NITin1 (5′-CCC AAT CGT TGT ACC GAA AG-3′) and NITin2 (5′-GAC GAA ACG ACG GAA CAA CT-3′), corresponding to the sequence of the pNIT2 insert; 5 μg of *G. pallidus* RAPc8 genomic DNA was digested by either *Eco*RI or *Hind*III in a 30-μl reaction. The digested DNA was size fractionated by electrophoresis and fragments in the size range 3–5 kb were isolated, purified and self-ligated in a 20-μl overnight reaction containing approximately 50 ng DNA.

Five microlitres of the ligation reaction was used in a 50-μl PCR reaction using a proof reading *Pfu* DNA polymerase (Promega, USA). The reaction conditions were: 94°C, 4 min, five cycles of 94°C, 30 s, 50°C, 30 s and 72°C, 4 min, five cycles of 94°C, 30 s, 58°C, 30 s and 72°C, 4 min, and 72°C, 10 min. The reaction was finally cooled to 4°C for 10 min. Following amplification, the reaction was incubated in the presence of *Taq* DNA polymerase in order to A tail the amplification product for downstream TA cloning. The ~4 kb

products were electrophoresed, gel purified and cloned into pGEM®-T Easy Vector Systems Kit (Promega, USA).

Random sequencing of library clones identified two plasmids, pINE2 (from the *Eco*RI restriction digest reaction) and pINH2 (from the *Hind*III restriction digest reaction), each containing overlapping portions of the nitrilase gene. Sequencing of the entire insert from each plasmid showed that the full nitrilase gene sequence and flanking regions were contained within the two plasmids.

Flanking sequence primers were designed to amplify and clone the ORF into pET29a vector in-frame. Pal-F (5′-CAT ATG GAG GGG AAG AAT ATG TC-3′) and Pal-R (5′-GGA TCC TTA ATT TTT CCA CTC AAT ATG TGT-3′) were used with the proofreading Accuzyme DNA polymerase (Bioline) to amplify the nitrilase ORF from the wild-type organism by a colony PCR (GeneBank Accession # of ORF DQ826045). The product was A-tailed and cloned into pGEM®-T Easy Vector Systems Kit (Promega, USA). The ORF was directionally cloned into pET29a into the NdeI site. The recombinant pET29a plasmid was electroporated into electrocompetent *E. coli* BL21(DE3)pLysS cells for expression.

Phylogenetic analysis of the gene sequence

Seventy-one nitrilase amino acid sequences were downloaded from Genbank (accession numbers shown on phylogenetic tree next to sequence ID: Fig. 2) and aligned with the *G. pallidus* RAPc8 sequence using Clustal X (Thompson et al. 1997). A maximum likelihood phylogentic tree (using model JTT) of aligned sequences (1000 iterations) was drawn using MEGA ver5 (Tamura et al. 2007).

Expression and purification

The recombinant nitrilase gene (cloned in pET29a) was expressed in *E. coli* BL21(DE3)pLys S with 1 mM IPTG (Roche, Germany) induction. Cells were sedimented by centrifugation at 4,000×*g* for 20 min at 4°C and resuspended in 50 mM Tris-HCl, pH 8.0 containing a protease inhibitor cocktail (Roche, Germany). Cells were disrupted by sonication (Misonix 3000, USA) and centrifuged at 20,000×*g* for 30 min at 4°C. The supernatant was filtered through a 0.22 μm filter and subjected to anion exchange chromatography using a Hiprep 16/10 Q XL Column (GE-Healthcare) equilibrated with 50 mM Tris-HCl, 100 mM NaCl pH 8.0 and eluted with 50 mM Tris-HCl, 1 M NaCl pH 8.0 at 5 ml min^{-1}.

Fractions containing the putative nitrilase based on band patterning on SDS PAGE gels, were pooled and concentrated by ultrafiltation using a 50 ml Amicon stirred cell with a molecular weight cut-off of 10 kDa (Millipore, USA). The concentrated protein fraction was separated by gel filtration on a Sephacryl S-300 HR gel filtration column (GE-Healthcare) equilibrated with 50 mM Tris-HCl, 200 mM NaCl pH 8.0. The column was calibrated with Biorad gel filtration standard which contained Thyroglobulin, bovine (670,000 Da), gamma-globulin, bovine (158,000 Da), ovalbumin, chicken (44,000 Da), myoglobulin, horse (17,000 Da) and Vitamin B12 (1,350 Da).

Nitrilase assays

Ammonia Assay The standard ammonia assay, as described in Almatawah et al. (1999), was used to measure activity during nitrilase purification. Substrates used (all at 5 mM) were benzonitrile, 4-cyanopyridine and 3-phenylproprionitrile. A unit of activity was defined as 1 μmole ammonia released per minute under standard assay conditions (at 37°C in 50 mM potassium phosphate buffer, pH 8). All assays were performed in triplicate.

HPLC Assays Reaction mixtures consisted of 750 μl of washed and induced whole cells added to 675 μl of a 50 mM Tris buffer, pH 8, and 75 μl of nitrile or amide substrate prepared in 100% methanol (substrate final concentration 5 mM). The final reaction volume was 1.5 ml. Reactions were incubated at 60°C for 10, 30 and 120 min with shaking (200 rpm), after which they were stopped by addition of 0.2 ml acidified acetonitrile: 0.1% (*v*/*v*) trifluoroacetic acid (TFA). Stopped reactions were centrifuged at 13,000×*g* for 10 min, filtered through a Cameo 25SS PES 0.22 μm filter (Osmonics) and 100 μl aliquots transferred into 2 ml high-performance liquid chromatography (HPLC) vials containing 900 μl 1:1 acetonitrile (ACN) and aqueous 0.1% (*v*/*v*) TFA. Control reactions in which enzyme was omitted from the reaction, were included.

Substrates (from Sigma-Aldrich, USA) were made up as 100 mM stock solutions in methanol. Benzonitrile, benzamide, mandelonitrile, 4-cyanopyrodine, 4-chlorobenzonitrile, hydrocinnamonitrile, and the equivalent amides were analysed by reversed-phase HPLC (RP-HPLC) using a Waters 2690 Separations Module equipped with a 996 Photodiode Array Detector. A 100×4.6 mm Chromolith Performance SpeedROD RP–18e column (Merck, Germany) was eluted isocratically at a flow rate of 0.5 ml/min by 6% $TFA_{(aq)}$: 40% ACN at 28°C, with sample injection volumes of 20 μl. The elution of substrates and nitrilase reaction products was monitored spectrophotometrically, and peak data extracted at 252 nm Integration and data analysis was done using Millennium Version 3.05.01 software (© 1998 Waters Corporation).

LC-Mass Spectral Analysis Coupled HPLC and mass spectral analysis was performed using the Waters Integrity™ System with photodiode array detector and Thermabeam™ mass detector. Mass spectral results of nitrile and amide standards were compared to internal library spectra from the Millennium Version 3.05.01 software (© 1998

Waters Corporation). Analyses were performed with an initial 15 min elution with 0.1% (*v*/*v*) formic acid at 0.2 ml min^{-1}, followed by 50% methanol: 50% acetonitrile for 2 min at 0.3 ml min^{-1}, 0.1% (*v*/*v*) formic acid for 5 min at 0.25 ml min^{-1} and 0.1% (*v*/*v*) formic acid for 8 min at 0.2 ml min^{-1}. The column temperature was set at 40°C.

Negative stain electron microscopy

Purified samples of *G. pallidus* RAPc8 nitrilase enzyme with a concentration of 0.5 mg ml^{-1} were pipetted onto glow discharged, carbon-coated copper grids and incubated at room temperature for 10 s. Grids was then blotted and washed twice prior to staining with 2% uranyl acetate and air-drying. Micrographs for image processing were recorded under low-dose conditions on a LEO912 transmission electron microscope operating at 120 kV. Images were captured at 50,000× magnification on a 2×2 k CCD camera with 14 μm pixels (Proscan, Germany). Captured images were examined using Boxer (Ludtke et al. 1999). Ring-like particles were selected in 128×128 pixel boxes at a sampling rate of 2.27 Å/pixel. A total of 4098 images

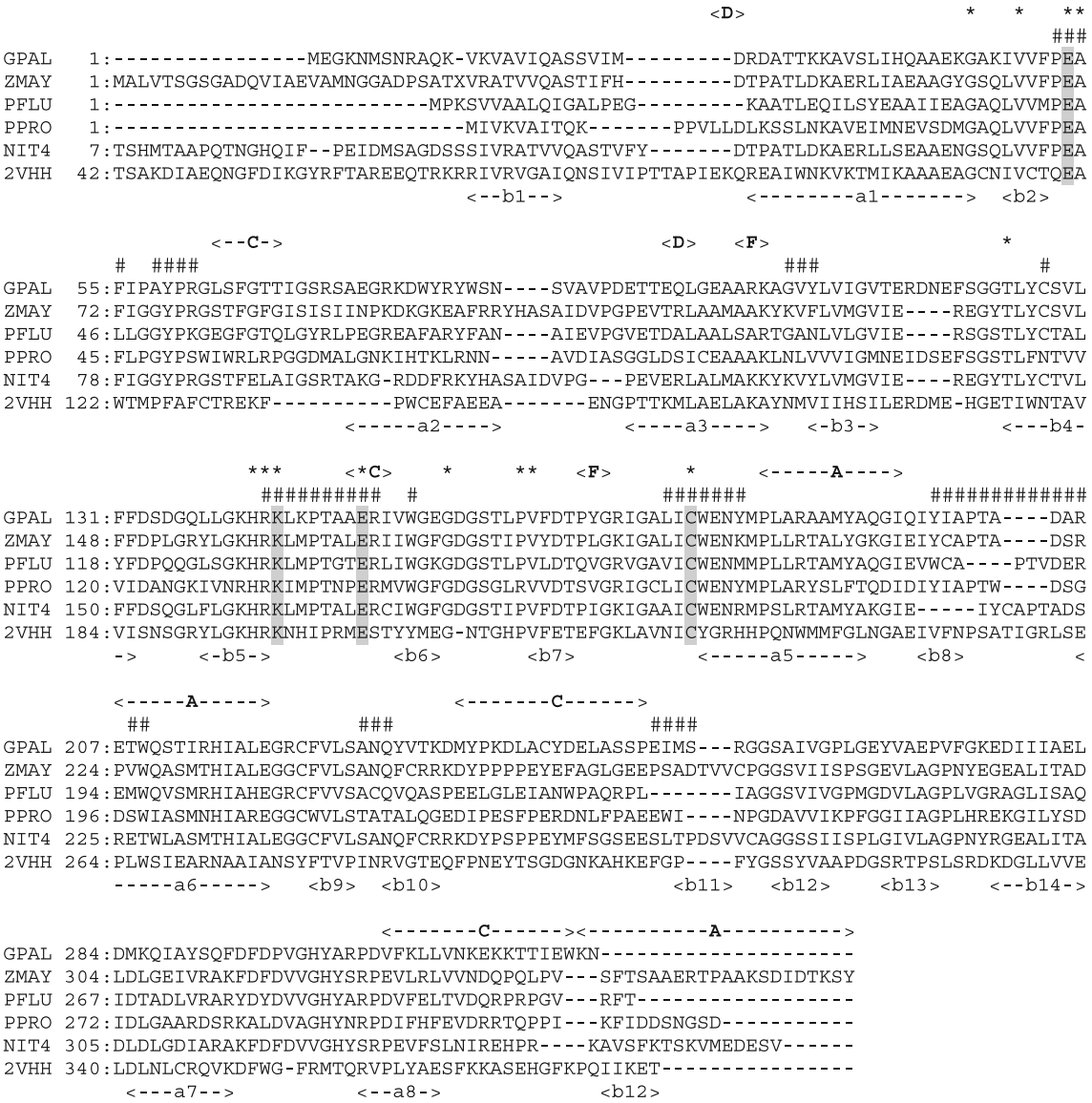

Fig. 1 Alignment of the *G. pallidus* RAPc8 nitrilase amino acid sequence to closest relatives. The closely related sequences are *Zea mays* (ZMAY), *Pseudomonas fluorescens* Pf5 (PFLU), *Photobacterium profundum* 3TCK (PPRO) and *Arabidopsis thaliana* (NIT4). The structure of the beta-alanine synthase from *Drosophila melanogaster* (2VHH) is one of those used in modelling the enzyme. It is the only homolog for which the C-surface structure is known. Conserved residues are denoted by "*asterisks*" and putative active site residues of the characteristic Glu, Lys, Glu, Cys catalytic tetrad are indicated in grey. Residues found within 11 Å of the active site Cys are denoted by "*number sign*". Alignment was based on the output of GenTHREADER (Jones 1999)

were captured. A total of 481 "figure-8" particles were selected in 256×256 pixel boxes. All selected particles were filtered and normalised to the same mean and standard deviation.

2D averaging

Image processing was performed using SPIDER (Frank et al. 1996). The ring structures were classified into 30

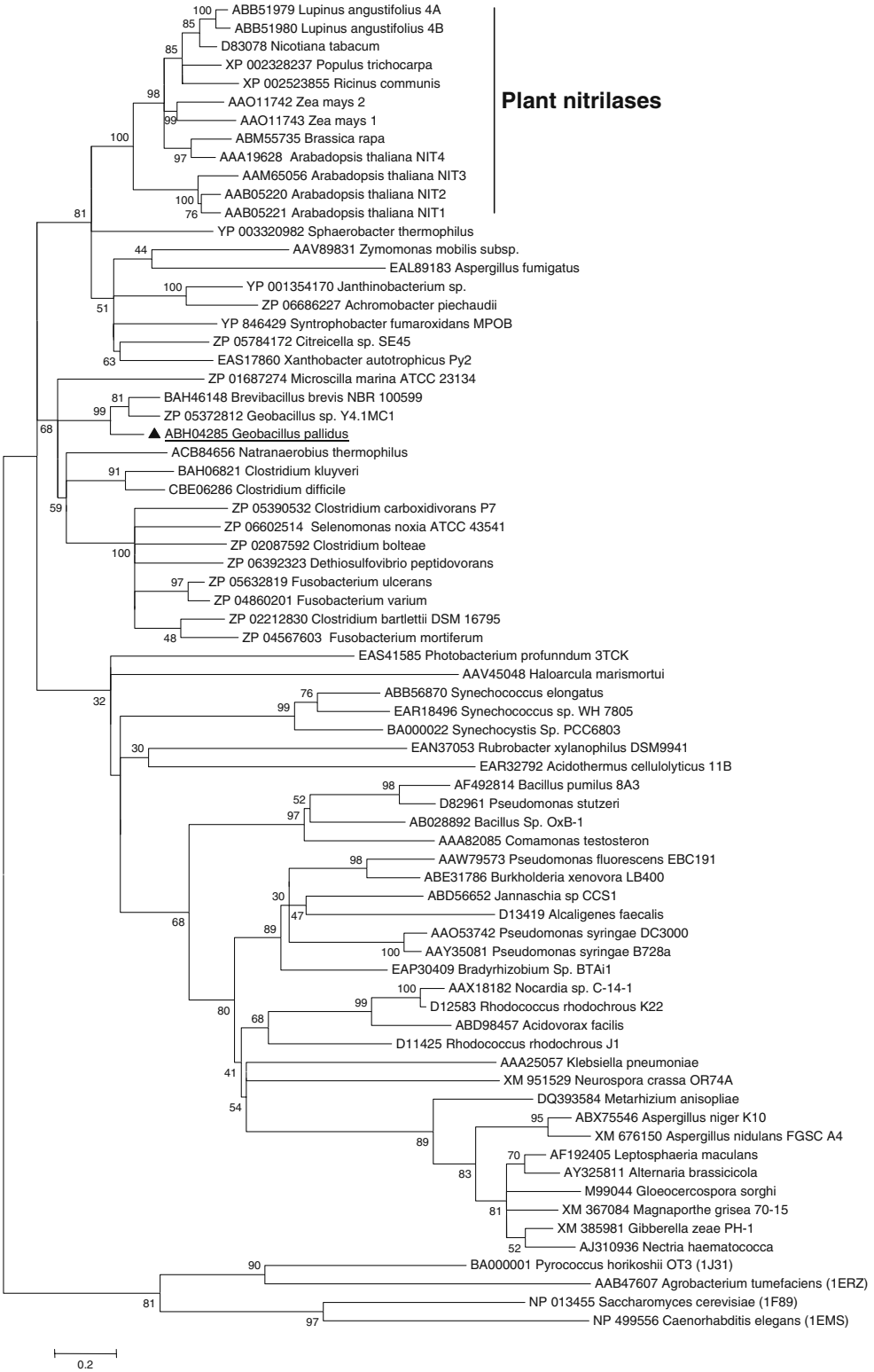

Fig. 2 A maximum likelihood phylogenetic tree of 71 known nitrilase protein sequences aligned with the *G. pallidus* RAPc8 nitrilase sequence using Clustal X (Thompson et al. 1997) and drawn using MEGA ver 5 (Tumara et al. 2007)

averages using rotationally invariant k-means (Penczek et al. 1996), and the classes were refined using multi-reference alignments (Joyeux and Penczek 2002) to exclude images that did not correlate. The "figure-8" images were averaged by reference-free alignment (Penczek et al. 1992) and this template was used to generate 5 class averages by rotationally invariant k-means and further refined by multi-reference alignment as described above.

Homology modelling

Homologs of the *G. pallidus* RAPc8 nitrilase with known structure were detected using GenTHREADER (Jones 1999; McGuffin and Jones 2003). Alignments were consolidated manually using the GenTHREADER output and predicted secondary structural features. Five templates (pdb codes:2w1v, 1uf5, 2vhh, 1j31 and 3hkx) were selected to build homology models of the nitrilase dimer using MODELLER (Sali and Blundell 1993; Fiser and Sali 2003). The energy of the models was minimised but no attempt was made to model loop insertions. Side chain conformations were adjusted using SCWRL4 (Krivov et al. 2009). Each model was evaluated using ProSA-web (Wiederstein and Sippl 2007) and by visual comparison to the templates using UCSF Chimera (Pettersen et al. 2004). Ultimately, a single model was selected on the basis of stereochemical consistency determined using MOLPROBITY (Davis et al. 2004, 2007).

Results

The isolated DNA sequence (Genbank ID: DQ826045) of the *G. pallidus* RAPc8 nitrilase was analysed and found to have a GC-content of 44% over the 972 bp ORF. The DNA melting temperature was calculated to be 82°C (Kibbe 2007). Analysis of the translated ORF sequence using Prosite (http://www.expasy.org) identified key motifs that are generally associated with nitrilases. These included the characteristic Glu, Lys, Cys catalytic triad, found at positions 53, 144 and 178, respectively. The conserved location of these key motifs is evident in alignments of the translated ORF against other nitrilase sequences (Fig. 1). The *G. pallidus* RAPc8 nitrilase monomer comprised 323 amino acids, with a calculated molecular weight of 35,790 Da and a theoretical pI of 6.16.

The amino acid sequence of the *G. pallidus* RAPc8 nitrilase had the highest protein sequence similarity to a nitrilase from *Geobacillus* sp. Y4.1MC1 (79%) and *Brevibacillus brevis* NBRC 100599 (78%). The *G. pallidus* RAPc8 nitrilase had ~63% amino acid similarity to nitrilases from *Natranaerobius thermophilus*, *Clostridium kluyveri* and *Clostridium difficile*. The plant nitrilases share between 46% and 53% amino acid identity to the *G. pallidus* RAPc8 nitrilase.

Phylogenetic analysis of the nitrilases indicates that nitrilases from *Geobacillus* sp., *Clostridium* sp., *Fusobacterium* sp, *Dethiosulfovibrio peptidovorans*, *Selenomonas noxia*, *N. thermophilus*, *B. brevis*, *Microscilla marina*, *Xanthobacter autotropicus*, *Synthtrophobacter fumaroxidans*, *Citreicella* sp., *Achromobacter piechaudaii*, *Janthinobacterium* sp., *Aspergillus fumigatus* and *Zymomonas mobilis* group with nitrilases from plants (Fig. 2). Electronic supplementary Fig. 1 shows a two-dimensional graphical representation of pair-wise amino acid sequence identities of the nitrilases. This plot emphasises the similarity of the grouped enzymes and clarifies their sequence relationship to the plant nitilases.

The enzyme was purified to homogeneity as demonstrated by SDS-PAGE (Fig. 3), by anion exchange chromatography followed by gel filtration chromatography. The nitrilase eluted from the calibrated gel filtration column with at an estimated native molecular weight of 600 kDa (data not shown), suggesting the functional multimeric form to be a 16-mer.

The hydrolysis of a range of nitriles was tested using the recombinant *G. pallidus* nitrilase (Table 1). Mass spectral analysis was used to confirm the nature of the nitrilase reaction products. While all the nitrile substrates tested (including benzonitrile) were converted, benzamide was not. Interestingly, the reaction products range from only the corresponding acid in the case of 4-cyanopyridine to almost entirely amide in the case of 3-phenylpropionitrile. 4-chlorobenzonitrile and mandelonitrile were converted with equal frequency to the corresponding amide or acid. At all time intervals tested, the substrates were converted to acid and amide products in an approximately constant ratio.

Negative stain EM showed heterogeneous isoforms for the *G. pallidus* RAPc8 nitrilase. The micrographs (Fig. 4) showed that both crescent shaped, c-shaped and closed ring-like structures were present. Larger "figure-8" particles

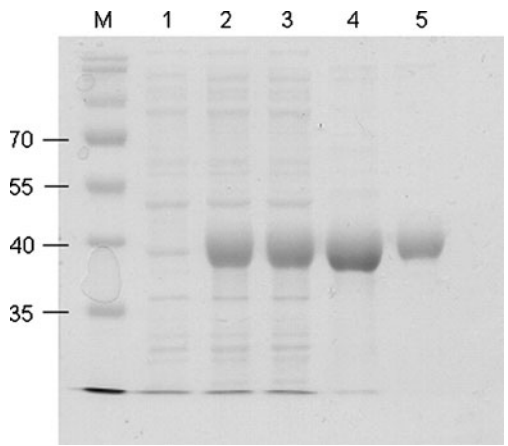

Fig. 3 SDS-PAGE of *G. pallidus* RAPc8 nitrilase during purification. *Lane M*, marker; *lane 1*, uninduced *E. coli* BL21; *lane 2*, IPTG induced cells; *lane 3*, cell-free supernatant; *lane 4*, anion exchange chromatography fraction; *lane 5*, gel filtration fraction

Table 1 Substrate specificity of *G. pallidus* RAPc8 nitrilase

Compound	Structure	Relative rate of substrate conversion	Acid : Amide (at 30 min)		Acid : Amide (at 120 min)	
Benzonitrile	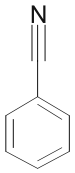	100	63	37	60	40
Benzamide	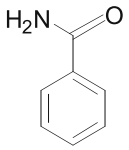	0	N/A		N/A	
R(+)-Mandelonitrile	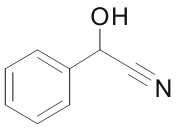	316	55	45	55	45
4-Cholorobenzonitrile	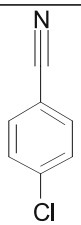	329	51	49	48	52
4-Cyanopyridine	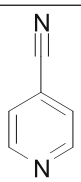	1138	100	0	100	0
Compound	**Structure**	**Relative rate of substrate conversion**	**Acid : Amide (at 10 min)***		**Acid : Amide (at 30 min)***	
3-Phenylpropionitrile	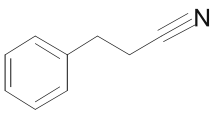	1650	10	90	11	89

Values are normalised to benzonitrile. Mass spectral analysis was used to confirm the identities of the amide and acid products

*The reaction was complete at 30 min therefore the data are shown at 10 min and 30 min respectively

(shown by white arrows in Fig. 4a) are also evident. It appears from the class averages shown in Fig. 5a that there are three distinct forms of open and closed ring-like structures. These class averages suggested progressive elongation of the oligomers, possibly representing stages in the assembly of the *G. pallidus* RAPc8 nitrilase, by the addition of dimers along the helical ramp until they terminate in the apparently closed, circular structure forming a "lock-washer". The "figure-8" structures appear to contain two of the "lock-washer" structures associated through the staggered ends.

The recent crystal structure of β-alanine synthase from *Drosophila melanogaster* (Lundgren et al. 2008) shows, at atomic resolution, how a nitrilase homologue can form an eight-monomer helical ramp. On the basis of a comparison with this structure (Fig. 5a I, II and III), we hypothesise that the *G. pallidus* RAPc8 nitrilase structures represent a hexamer, an octamer and a decamer, respectively. We were

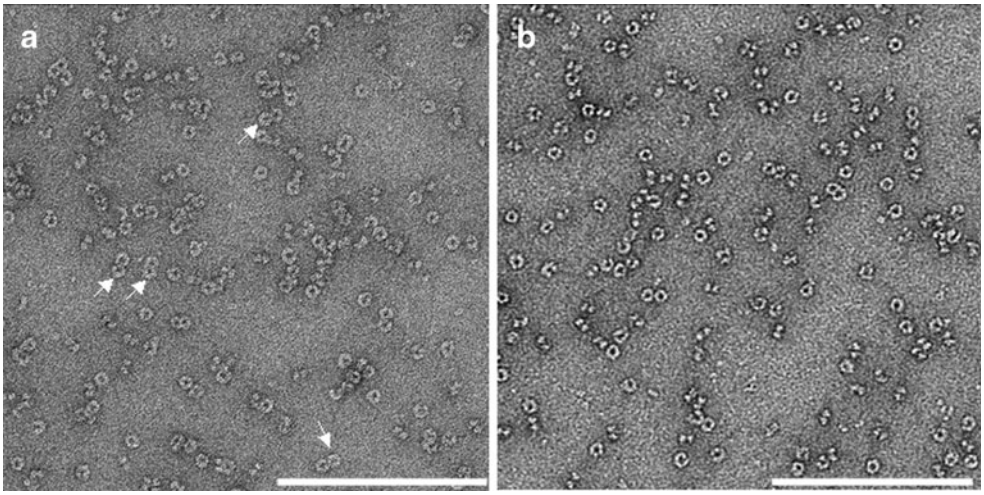

Fig. 4 Transmission electron micrographs of purified *G. pallidus* RAPc8 nitrilase. **a** Enzyme preparation "figure-8" structures (*white arrows*); **b** preparation in which closed rings are the major form

also able to identify classes which probably correspond to the structures I, II and III viewed from the side (Fig. 5a, IV–VI).

A further precedent for the existence of c-shaped helical ramps in microbial nitrilases occurs in *Rhodococcus rhodochrous* J1 (Thuku et al. 2007). In this case, the helical symmetry parameters of the C-terminal truncated nitrilase from *R. rhodochrous* J1 have an axial rise per dimer (Δz) of 15.8 Å and a rotation per dimeric subunit (Δφ) of −73.5° (Thuku et al. 2007). If our conclusions concerning the number of subunits in each of the classes is correct, then there is sufficient information in the depicted views to estimate the axial rise per dimer (Δz) as well as the rotation per subunit (Δφ). The axial rise was calculated to be 15±1 Å by measuring the stagger in the side-views (Fig. 5, IV and V). The rotation per dimeric subunit was calculated by measuring the outside angle of the top-views divided by the predicted number of dimers in the isoform (Fig. 5: I and II). The two angles measured produced an average rotation angle of −75°±1°. The outer radius of the *G. pallidus* RAPc8 spiral was also measured from the top-views to be 47±1 Å.

Discussion

The gene encoding the *G. pallidus* RAPc8 nitrilase was cloned and sequenced. This bacterial nitrilase showed

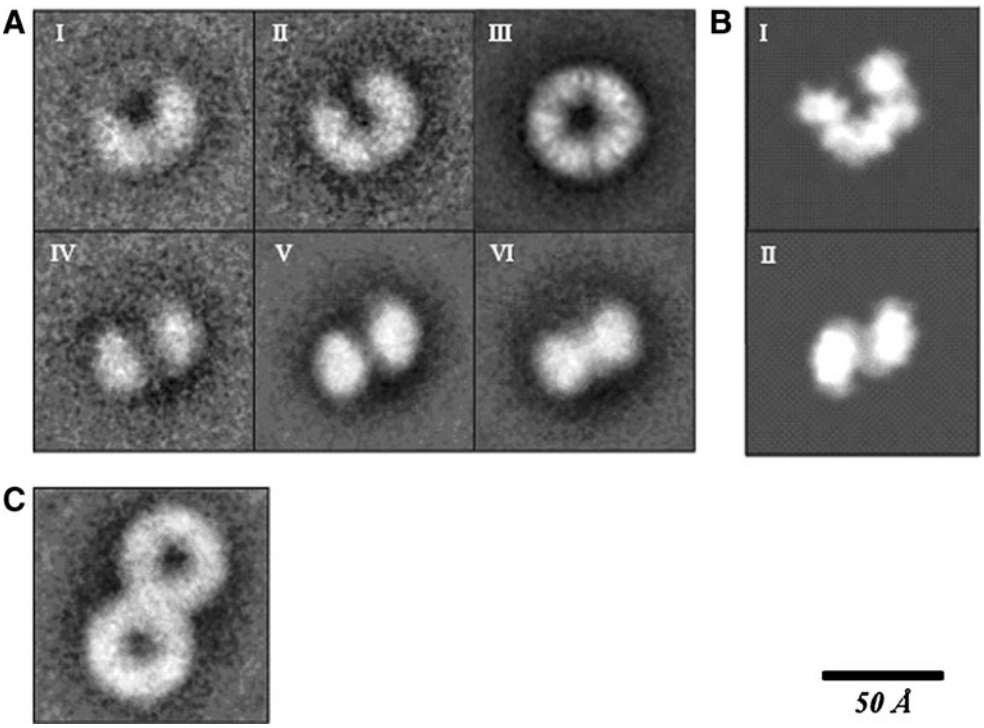

Fig. 5 Class averages representing common particle views produced by iterative classification and alignment of isolated particle images. **a** Depicts top (*I–III*) and corresponding side views (*IV–VI*) of three distinct isoforms showing the open and closed ring-like structure. These possibly represent a hexamer, octamer and decamer (or above), respectively. **b** shows the projections determined from the deposited co-ordinates of beta-alanine synthase from *D. melanogaster* (Lundgren et al. 2008) generated using SPIDER (Frank et al. 1996). **c** Shows the "figure-8" class average which is likely to represent two decamers which have associated in opposite orientations

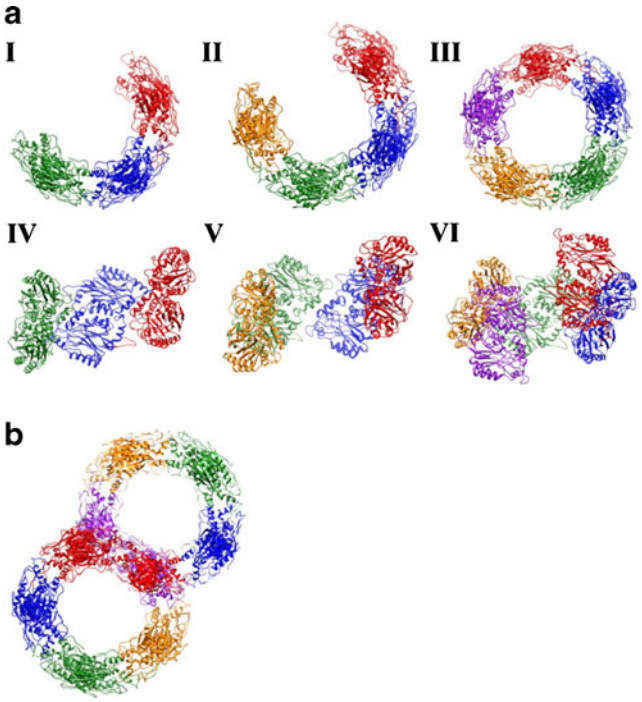

Fig. 6 Oligomers of *G. pallidus* RAPc8 nitrilase interpreted from 2D averaging and constructed by applying the axial shift and helical twist determined from the images, to a dimeric homology model of the nitrilase. **a** Top (*I–III*) and corresponding side views (*IV–VI*) of three distinct isoforms are represented by a hexamer, octamer and decamer. **b** Model of the "figure-8" form. Image visualised using UCSF Chimera (Pettersen et al. 2004; Goddard et al. 2005)

greater sequence similarity to plant nitrilases than to many other bacterial nitrilases. The result supports the proposal by Pace and Brenner (2001) and Podar et al. (2005) that horizontal gene transfer events between the eukaryotic and prokaryotic kingdoms as a consequence of ecological association account for the phylogenetic positions of nitrilase genes (Fig. 2). Not only does prokaryotic nitrilase phylogeny not reflect the taxonomy of the host organism, but nitrilases are found amongst clusters of other genes which are separated by few or no intergenic nucleotides (Podar et al. 2005). Such genomic structures are consistent with large transposed genetic elements.

The purified enzyme had an apparent mean molecular weight of 600 kDa as determined by size exclusion chromatography. With a molecular weight of 35,790 Da, an average composition of 16.8 (17) monomers per multimer is suggested. However, electron microscopy and image classification showed a range of structural forms in purified enzyme preparations, including crescent-like, "c-shaped", circular and "figure-8" shapes. Structural models (Fig. 6) based on the principles elaborated by Thuku et al. (2009) suggested that these forms contained 6, 8, 10 and 20 subunits, respectively, equivalent to native molecular weights of 215, 286, 358 and 716 kDa. Longer helices were not seen in the micrographs. The absence of such longer forms suggests that an interaction which occurs at the ten-monomer "lock-washer" stage causes termination of the helical ramp. This situation is analogous to the 14-monomer, self-terminating spirals seen in the cyanide dihydratase from *Pseudomonas stutzeri* AK61 (Sewell et al. 2003). The existence of the "figure-8" form is interesting. These structures can be formed using the same inter-molecular interactions as occur in the spiral ramps by mating two "lock-washers" and thus form a completely closed structure.

Similar to several plant nitrilases and some bacterial nitrilases, the *G. pallidus* RAPc8 nitrilase produced both acid and amide products from aromatic nitrile conversions (Table 1). The relative rates of these conversions suggest that a combination of electron activating effects (enhanced electropositivity of the nitrile carbon by addition of electron-withdrawing groups) and steric hinderance (that is, distance of the nitrile carbon from a bulky group) may play a role but it is necessary to do further kinetic analysis to separate the different effects.

Product analysis data showed large variations in the ratios of acid to amide products. One possibility is that these values could be dictated by the relative kinetics of the two water additions (that is, the ratio k_1/k_2) in a sequential ("in series") reaction pathway [I]:

$$\mathrm{R-CN+H_2O} \xrightarrow{k_1} \mathrm{R-CONH_2+H_2O} \xrightarrow{k_2} \mathrm{R-COOH+NH_3} \quad \text{(I)}$$

In such a case, the amide/acid ratio would be expected to decrease with reaction time, particularly with $k_1 > k_2$. We

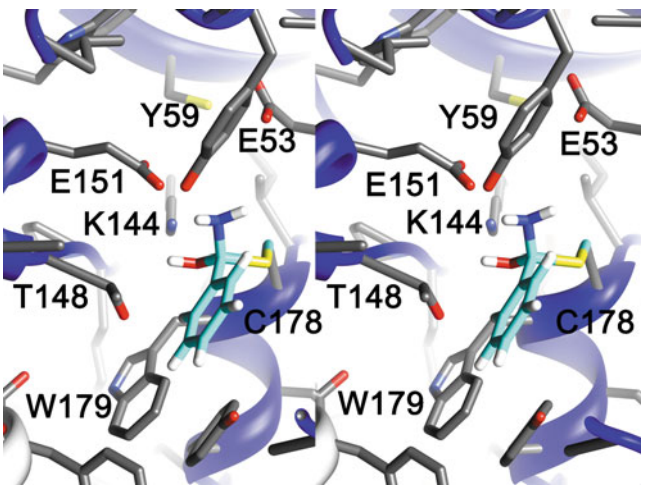

Fig. 7 A stereo view of the putative tetrahedral intermediate on C178 that would be formed as a transition state during the conversion of benzonitrile to benzoic acid. The homology model locates the neighbouring amino acid side chains: E53, Y59, K144, T148, E151 and W179 are labelled. Note the proximity of K144 and E151 to the amino group

noted, however, that the amide:acid ratios were generally constant throughout the reaction period, an observation which is not consistent with an 'in series' reaction profile.

The apparently anomalous results obtained from use of the benzonitrile/benzamide substrate pair also suggests that the reaction pathway may not be "in series". The absence of any detectable hydrolysis of benzamide suggests that there is no benzamide intermediate and that addition of the second water molecule is dependent on electronic events which are a function of the first water addition. The difference between the two reaction routes is also thought to depend on which bond in the tetrahedral intermediate (following the postulated thioimidate complex) breaks (Jandhyala et al. 2005).

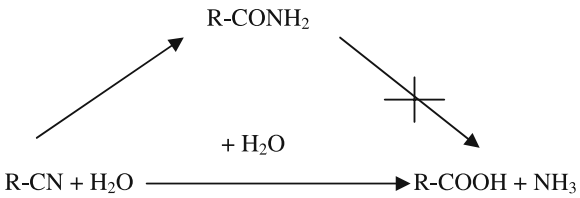

(II)

Detailed examination of the tetrahedral intermediate provides insight into factors that have a bearing on the acid: amide ratio. Two tetrahedral adducts at the active site cysteine which can be used to model the tetrahedral intermediate have been visualised by X-ray crystallography, namely the cacodylate adduct of XC1258 from *Xanthomonas campestris* (Chin et al. 2007) (pdb:2e11) and the acetohydroxamic acid derivative of the amidase from *Pseudomonas aeruginosa* (Andrade et al. 2007) (pdb:2uxy). The tetrahedral carbon forms bonds to the active site cysteine, a tetrahedral amine, a hydroxyl and the substrate R-group (Fig. 7). The model suggests stereoselective formation of an intermediate with an S-configuration. Thereafter, the steps leading to acid formation involve the amine group leaving and the formation of a thioester, which hydrolyses. The alternative is that the cysteine is the leaving group in which case the product is the amide. Although there are a number of factors to consider regarding leaving group selectivity, in the absence of assistance one would expect the cysteine to preferentially leave as the C–S bond is much weaker than the C-N bond. The results in Table 1, however, suggest that a π-electron-withdrawing R-group switches the expected amide formation to that of acid, possibly because the sulphur offers a greater mesomeric stabilisation of incipient carbocationic character in the transition state.

Simple homology modelling (Fig. 7) suggests the residues adjacent to the tetrahedral adduct at C178 in the case of *G. pallidus* RAPc8 nitrilase are E53, E151 and K144 which are always conserved and T148, Y59 and W179 which are widely conserved. Our model locates both E151 and K144 in the immediate vicinity of the amino group. It is possible that the proximity of the lysine would assist the amino leaving group via acid catalysis. While the location of these residues provide no obvious solution to a mechanism for "product specificity", we speculate that subtle details of the immediate electronic environment of the tetrahedral intermediate dictate the relative rates of N–C bond or S–C bond cleavage.

This point is emphasised by the observation by Kaplan et al. (2006) who found that the nitrilase from *Aspergillus niger* K10 produced a substantially greater proportion of amide when hydrolysing 4-cyanopyridine than it did in the case of benzonitrile, essentially the inverse of the result we obtained with the enzyme from *G. pallidus* RAPc8.

The influence of the immediate environment is further highlighted by the experiments of Sosedov et al. 2010. Mutational analysis of residues adjacent to the catalytic C164 in the *Pseudomonas fluorescens* EBC191 nitrilase resulted in increased amide formation and enantioselectivity. In particular, the C163N, C163Q and T110I-C163N enzyme variants produced 70% (*R*)-mandelic acid and 59% (*S*)-mandeloamide from (R,S)-mandelonitrile. Similarly, 16% more (*R*)-2-phenylpropionionamide was produced by the A165R mutant compared to the wild type enzyme (Kiziak and Stolz 2009). These results indicate further complexity in that the enantiomer of the substrate plays a role in determining whether the amide or acid product is produced.

Although we were initially prompted to examine the amide production of the *G. pallidus* RAPc8 nitrilase because of the similarity of the sequence at the active site cysteine (ICWEN) to that of *Arabidopsis thaliana* NIT4 (Piotrowski et al. 2001), it appears from the analysis presented in Fig. 2 that overall sequence similarity is a poor indicator of product specificity. It is now clear that detailed structural information is necessary for better understanding of the mechanism of these enzymes.

Acknowledgements We would like to thank Roger Hunter for stimulating discussions concerning the chemistry of the tetrahedral intermediate. DW was supported by a NRF and DAAD bursary. KD was supported by a Harry Crossley fellowship. Much of the work was funded by the Carnegie Corporation of New York through the Joint UCT/UWC Masters programme in structural biology. DAC also thanks the South African National Research Foundation (Institutional Research Development Program) for financial support. AV was supported by the Carnegie Corporation of New York.

References

Almatawah QA, Cramp R, Cowan DA (1999) Characterization of an inducible nitrilase from a thermophilic bacillus. Extremophiles 3:283–291

Andrade J, Karmali A, Carrondo MA, Frazao C (2007) Structure of amidase from Pseudomonas aeruginosa showing a trapped acyl transfer reaction intermediate state. J Biol Chem 282:19598–19605

Brady D, Beeton A, Zeevaart J, Kgaje C, van Rantwijk F, Sheldon RA (2004) Characterisation of nitrilase and nitrile hydratase biocatalytic systems. Appl Microbiol Biotechnol 64:76–85

Brady D, Dube N, Pettersen R (2006) Green chemistry: highly selective biocatalytic hydrolysis of nitrile compounds. S Afr J Sci 102:339–344

Brenner C (2002) Catalysis in the nitrilase superfamily. Curr Opin Structl Biol 12:775–782

Chin KH, Tsai YD, Chan NL, Huang KF, Wang AH, Chou SH (2007) The crystal structure of XC1258 from *Xanthomonas campestris*: a putative procaryotic Nit protein with an arsenic adduct in the active site. Proteins 69:665–671

Davis IW, Murray LW, Richardson JS, Richardson, DC (2004) MOLPROBITY: structure validation and all-atom contact analysis for nucleic acids and their complexes. Nucleic Acids Res 32(Web Server issue): W615–W619

Davis IW, Leaver-Fay A, Chen VB, Block JN, Kapral GJ, Wang X, Murray LW, Arendall WB 3rd, Snoeyink J, Richardson JS, Richardson DC (2007) MolProbity: all-atom contacts and structure validation for proteins and nucleic acids. Nucleic Acids Res 35(Web Server issue): W375–W383

Fernandes BCM, Mateo C, Kiziak C, Chmura A, Wacker J, van Rantwijk F, Stolz A, Sheldon RA (2006) Nitrile hydratase activity of a recombinant nitrilase. Adv Synth Catal 348:2597–2603

Fiser A, Sali A (2003) MODELLER: generation and refinement of homology-based protein structure models. Methods Enzymol 374:463–493

Frank J, Radermacher M, Penczek P, Zhu J, Li Y, Ladjadj M, Leith A (1996) SPIDER and WEB: processing and visualization of images in 3D electron microscopy and related fields. J Struct Biol 116:190–199

Jandhyala D, Willson RC, Sewell BT, Benedik MJ (2005) Comparison of cyanide-degrading nitrilases. Appl Microbiol Biotechnol 68:327–335

Jones DT (1999) GenTHREADER: an efficient and reliable protein fold recognition method for genomic sequences. J Mol Biol 287:797–815

Joyeux L, Penczek PA (2002) Efficiency of 2D alignment methods. Ultramicroscopy 92:33–46

Kaplan O, Vejvoda V, Plíhal O, Pompach P, Kavan D, Bojarová P, Bezouska K, Macková M, Cantarella M, Jirků V, Kren V, Martínková L (2006) Purification and characterization of a nitrilase from *Aspergillus niger* K10. Appl Microbiol Biotechnol 73:567–575

Kibbe WA (2007) OligoCalc: an online oligonucleotide properties calculator. Nucleic Acids Res 35:W43–46

Kimani SW, Agarkar VB, Cowan DA, Sayed MF, Sewell BT (2007) Structure of an aliphatic amidase from *Geobacillus pallidus* RAPc8. Acta Crystallogr D Biol Crystallogr 63:1048–1058

Kiziak C, Stolz A (2009) Identification of amino acid residues responsible for enantioselectivity and amide formation capacity of the arylacetonitrilase from *Pseudomonas fluoroscens* EBC191. Appl Environ Microbiol 75:5592–5599

Krivov GG, Shapovalov MV, Dunbrack RL Jr (2009) Improved prediction of protein side-chain conformations with SCWRL4. Proteins 77:778–795

Ludtke SJ, Baldwin PR, Chiu W (1999) EMAN: semiautomated software for high-resolution single-particle reconstructions. J Struct Biol 128:82–97

Lundgren S, Lohkamp B, Andersen B, Piskur J, Dobritzsch D (2008) The crystal structure of B-alanine synthase from *Drosophila melanogaster* reveals a homo-octameric helical turn-like assembly. J Mol Biol 377:1544–1559

McGuffin LJ, Jones DT (2003) Improvement of the GenTHREADER method for genomic fold recognition. Bioinformatics 19:874–881

O'Reilly C, Turner PD (2003) The nitrilase family of CN hydrolysing enzymes—a comparitive study. J Appl Biol 95:1161–1174

Pace HC, Brenner C (2001) The nitrilase superfamily: classification, structure and function. Genome Biol 2:1–9

Penczek PA, Radermacher M, Frank J (1992) Three-dimensional reconstruction of single particles embedded in ice. Ultramicroscopy 40:33–53

Penczek PA, Zhu J, Frank J (1996) A common-lines based method for determining orientations for N>3 particle projections simultaneously. Ultramicroscopy 63:205–218

Pereira RA, Graham D, Rainey FA, Cowan DA (1998) A novel thermostable nitrile hydratase. Extremophiles 2:347–357

Pettersen EF, Goddard TD, Huang CC, Couch GS, Greenblatt DM, Meng EC, Ferrin TE (2004) UCSF Chimera—a visualization system for exploratory research and analysis. J Comput Chem 25:1605–1612

Piotrowski M, Schönfelder S, Weiler EW (2001) The *Arabidopsis thaliana* isogene NIT4 and its orthologs in Tobacco encode β-cyano-L-alanine hydratase/nitrilase. J Biol Chem 276:2616–2621

Podar M, Eads JR, Richardson TH (2005) Evolution of a microbial nitrilase gene family: a comparative and environmental genomics study. BMC Evol Biol 5:42

Sali A, Blundell TL (1993) Comparative protein modelling by satisfaction of spatial restraints. J Mol Biol 234:779–815

Sewell BT, Berman MN, Meyers PR, Jandhyala D, Benedik MJ (2003) The cyanide degrading nitrilase from *Pseudomonas stutzeri* AK61 Is a two-fold symmetric, 14-subunit spiral. Structure 11:1413–1422

Sosedov O, Baum S, Burger S, Kathrin M, Kiziak C, Stolz A (2010) Construction and application of variants of the *Pseudomonas fluorescens* EBC191 arylacetonitrilase for increased production of acids or amides. Appl Environ Microbiol 76:3668–3674

Tamura K, Dudley J, Nei M, Kumar S (2007) MEGA4: Molecular Evolutionary Genetics Analysis (MEGA) software version 4.0. Molecular Biology and Evolution 24:1596–1599

Thompson JD, Gibson TJ, Jeanmougin F, Higgins DG (1997) The ClustalX windows interface: flexible strategies for multiple sequence alignment aided by quality analysis tools. Nucleic Acids Res 25:4876–4882

Thuku RN, Weber BW, Varsani A, Sewell BT (2007) Post-translational cleavage of recombinantly expressed nitrilase from *Rhodococcus rhodochrous* J1 yields a stable, active helical form. FEBS J 274:2099–2108

Thuku RN, Brady D, Benedik MJ, Sewell BT (2009) Microbial nitrilases: versatile, spiral forming, industrial enzymes. Appl Microbiol 106:703–727

Wiederstein, M and Sippl, MJ (2007) ProSA-web: interactive web service for the recognition of errors in three-dimensional structures of proteins. Nucleic Acids Res 35(Web Server issue): W407–W410